Shahrood University of Technology
Iranian Society of Mining Engineering (IRSME)
Journal of Mining and Environment (JME)
journal homepage: www.jme.shahroodut.ac.ir
THOMSON REUTERS

Developing New Models for Flyrock Distance Assessment in Open-Pit Mines

Jamshid Shakeri[1], Hasel Amini Khoshalan[1*], Hesam Dehghani[2], Marc Bascompta[3] Kennedy Onyelowe[4]

1. Department of Mining Engineering, Faculty of Engineering, University of Kurdistan, Sanandaj, Iran
2. Department of Mining Engineering, Hamedan University of Technology, Hamedan, Iran
3. Department of Mining Engineering, Polytechnic University of Catalonia, Barcelona, Spain
4. Department of Civil Engineering, Michael Okpara University of Agriculture, Umudike, Nigeria

Article Info

Received 8 April 2022
Received in Revised form 21 April 2022
Accepted 28 April 2022
Published online 28 April 2022

DOI:10.22044/jme.2022.11805.2170

Keywords

Flyrock distance
Linear multivariate regression
Imperialist competitive algorithm
Adaptive neuro-fuzzy inference system
Artificial neural network

Abstract

In this research work, a comprehensive study is conducted to predict flyrock as a typical and undesirable phenomenon occurring during the blasting operation in open-pit mining. Despite the availability of several empirical methods for predicting the flyrock distance, the complexity of flyrock analysis has resulted in the low performance of these models. Therefore, the statistical and robust artificial intelligence techniques are applied for flyrock prediction in the Sungun copper mine in Iran. For this purpose, the linear multivariate regression (LMR), imperialist competitive algorithm (ICA), adaptive neuro-fuzzy inference system (ANFIS), and artificial neural network (ANN) methods are applied to predict flyrock with effective parameters including the blasthole diameter, stemming, burden, powder factor, and maximum charge per delay. According to the attained results, the ANN model with the structure of 5-8-1, Levenberg-Marquardt as the learning algorithm, and log-sigmoid (logsig) as the transfer functions are selected as the optimal network with the RMSE and R2 values of 5.04 m and 95.6% to predict flyrock, respectively. Also it can be concluded that the ICA technique has a relatively high capability in predicting flyrock, with the LMR and ANFIS models placed in the next. Finally, the sensitivity analysis reveal that the powder factor and blasthole diameters have the most importance on the flyrock distance in the present work.

1. Introduction

Despite extensive advances in the industry of drilling machinery, blasting has still a significant role in extracting the mineral resources [1]. In this respect, by an accurate and optimal blasting, the productivity can be improved the and total costs can be increased. The researches have shown that around two thirds of total blasting energy is wasted due to the adverse and harmful phenomena caused by the blasting such as flyrock, air-blast, and ground vibration, and the rest is spent for rock fragmentation [1-6]. Flyrock is an environmental problem defined as throwing or displacement of rock pieces outside the normal distances from the blast area due to wasting of explosive energy, which can lead to fatalities in mines [7, 8]. Therefore, the evaluation and estimation of flyrock is vital to minimize these problems. According to Figure 1, flyrock can be divided into the three main categories of face bursting, rifling, and cratering.

Based on the previous studies, controllable and uncontrollable parameters can affect flyrock [9]. The controllable parameters include the powder factor, burden, stemming, hole spacing, stemming length, hole length, hole diameter, sub-drilling, and so forth. On the other hand, the uncontrollable parameters include the rock mass characteristics and geological structures including the bedding planes, faults, and joints [10]. Given the importance of investigating the blasting-induced flyrock in mines and construction projects, several researchers have studied the rate of blasting-induced flyrock. Some researchers have developed

Corresponding author: h.amini@uok.ac.ir (J. Shakeri).

empirical models to predict the flyrock distance. According to Lundborg *et al*. [11], the flyrock distance can be determined by the following equation:

$$L_m = 260 \times D^{2/3} \quad (1)$$

where L_m is the maximum flyrock distance in m and D is the blasthole diameter in inch.

One of the other empirical models for prediction of flyrock (F) has been introduced by Ghsemi *et al*. [9], where the effective parameters including burden (B), spacing (S), stemming (St), blasthole length (H), blasthole diameter (D), charge per blasthole (Q), and powder factor (P) are considered as follow:

$$F = 6946.547[B^{-0796} S^{0.783} St^{1.994} H^{1.649} D^{1.766} (P/Q)^{1.465}] \quad (2)$$

Dehghani and Shafaghi [12] have predicted the blasting-induced flyrock distance using the dimensional analysis (DA) algorithm and the differential evaluation (DE) algorithm. The results obtained have presented that the offered DE-DA model outperforms the experimental approaches. Koopialipoor *et al*. [8] have used GA-ANN, particle swarm optimization (PSO)-ANN, and imperialist competitive algorithm (ICA)-ANN in order to predict the flyrock distance produced by blasting. According to their results, the PSO-ANN model has more ability than the other models for prediction of flyrock. Lu *et al*. [13] have developed machine learning models to predict the flyrock produced by blasting. They collected and used data from three granite mines in Malaysia. According to their results, the machine learning models outperform ANN and multiple regression models. Rad *et al*. [14] have used a recurrent fuzzy neural network (RFNN) with a genetic algorithm (GA) for flyrock prediction. In this study, non-linear regression, ANN, and hybrid ANN-GA models were applied to evaluate the suitability of the RFNN-GA model. The results obtained showed that the proposed RFNN-GA model had a better performance in flyrock prediction. Han *et al*. [15] have used the random forest method and the Bayesian network (BN) method with an acceptable performance. Nguyen *et al*. [16] have presented a numerical model for estimation of flyrock using a powerful combination of Kernel functions, support vector machine (SVM), and whale optimization algorithm (WOA). Zhou *et al*. [17] have used the non-linear and Monte Carlo (MC) simulation models for predicting and simulating flyrock. The results of the MC simulation showed the good accuracy of flyrock distance. Manjezi *et al*. [18] have used the ANN, LMR, and Gene Expression Programming (GEP) models to predict flyrock. The results of their studies show that the GEP model has a good accuracy in predicting flyrock.

Regarding the mentioned points, the present work aimed to use the statistical and intelligent methods to assess the rate of blasting-induced flyrock in the Sungun copper mine using a statistical relationship. In this work, for the first time, the statistical relationships using linear multivariate regression and ICA are proposed. Furthermore, the results obtained are compared with ANN and ANFIS in the Sungun copper mine.

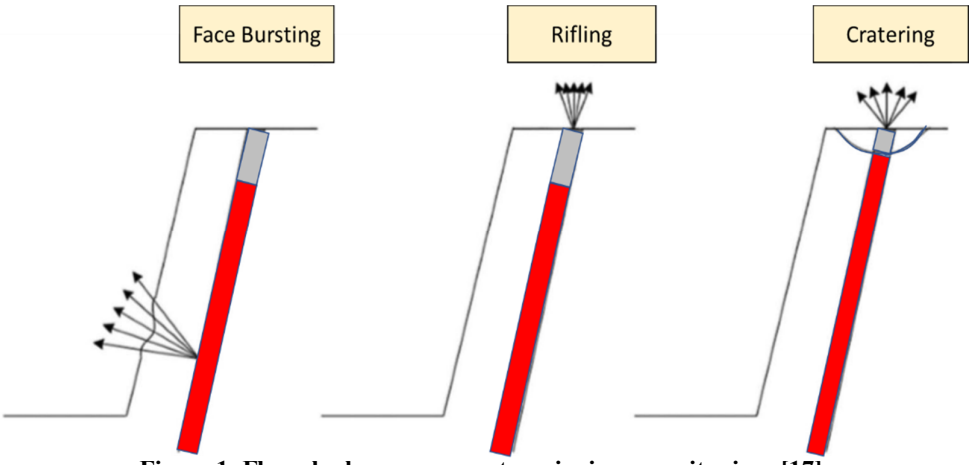

Figure 1. Flyrock phenomenon categories in open-pit mines [17].

2. Data and Methods

2.1. Database

As the largest copper mine located in NW Iran, the Sungun copper open-pit mine has a confirmed ore reserve of about 1600 Mt with an average grade of 0.67% copper. In the Sungun mine, the blasting operations are performed by ANFO, detonating cord and Nonel systems. The flyrock caused by the blasting operation is one of the unwanted phenomena in this mine, for which a maximum of 100 m flyrock distance has been reported (Figure 2).

According to the performed studies, a comprehensive database consisting of 281 datasets with five effective input parameters was prepared for predicting the flyrock (FR). Table 1 demonstrates the range of the input and output parameters applied in this work. Also the relationship between the input and output parameters, as the Pearson's correlation matrix, is shown in Table 2. It is notable to mention that RMR of the considered rocks in the present study is about 40.

Figure 2. A view of Sungun copper mine in Iran.

Table 1. Considered input and output parameters.

Input/ output	Parameter	Symbol	Min	Max	Mean	Std. Deviation
Inputs	Hole diameter (in)	D	3	5.5	5.178	0.532
	Burden (m)	B	2.5	5	4.090	0.552
	Stemming (m)	St	2.5	5.5	3.922	0.505
	Powder factor (Kg/ton)	Pf	0.18	1	0.425	0.115
	Charge per delay (Kg/ms)	Ch	9.23	88	24.088	13.375
Output	Flyrock (m)	FR	13	100	67.320	21.027

In order to find the best relationship between the considered inputs data and the flyrock distance as the output parameters, 70% of the data was randomly considered as the learning data, while the rest of the data was used to validate the proposed statistical relationship.

Table 2. Matrix of Pearson's correlation for applied inputs and output parameters.

Correlations	D	B	St	Pf	Ch	FR
D	1	0.565	0.600	0.210	0.058	0.054
B	0.565	1	0.787	-0.504	0.051	-0.583
St	0.600	0.787	1	-0.208	0.127	-0.120
Pf	0.210	-0.504	-0.208	1	0.071	0.674
Ch	0.058	0.051	0.127	0.071	1	0.066
FR	0.054	-0.583	-0.120	0.674	0.066	1

According to the linear dependence degree in Table 2, the value 0 indicates no correlation, whilst the values -1 and 1 show a negative and a positive correlation between the parameters, respectively [19].

2.2. Methodology

In the present work, the linear multivariate regression modeling and the intelligent methods of ANN, ICA, and ANFIS were studied for predicting the flyrock produced by blasting in the Sungun

copper mine. This section gives an overview of these methods.

2.2.1. Linear multivariate regression

The linear multivariate regression (LMR) is a statistical method that uses several explanatory variables for predicting the outcome of a response variable. An LMR model with n regression variables can be expressed as follows:

$$C = \beta_0 + \beta_1 x_1 + ... + \beta_n x_n + \varepsilon \quad (3)$$

where β_0 is the constant value, β_i is the regression coefficients $(i = 1, 2, ..., n)$, and ε is the model's error value.

By considering the prediction models of complex structures, the following nonlinear model can be applied [5, 20-22]:

$$C = \beta_0 + \beta_1 x_1 + \beta_2 x_2^3 + \beta_3 e^{x_3} + \beta_4 x_1 x_2 + \varepsilon \quad (4)$$

In order to simplify this non-linear model, the linear variables can be simply substituted. Thus by taking $z_1 = x_1$, $z_2 = x_2^3$, $z_3 = e^{x_3}$ and $z_4 = x_1 x_2$, Equation (4) can be expressed as the following form in order to predict the flyrock values:

$$C = \beta_0 + \beta_1 z_1 + \beta_2 z_2 + \beta_3 z_3 + \beta_4 z_4 + \varepsilon \quad (5)$$

2.2.2. Imperialist competitive algorithm (ICA)

The ICA method has been developed as a global search strategy applying the sociopolitical evolution of humans as a basis of inspiration [23]. High speed of convergence and more capability of searching global optimization are the advantages of this method [24, 25]. According to Figure 3, which shows the process of this algorithm, initialize the empires (including countries) as the random population is the first step [26, 27]. In the following, some of the powerful counties according to their cost function in the produced population are considered as the imperialists, and the rest as the colonies. Based on the power of each imperialist, the colonies are allocated among them.

In the next step, after moving the colonies to their imperialist country, the imperialistic competition occurs among the empires. Consequently, the powerful empires remains, and the weaker ones will be eliminated, and their colonies will belong to the powerful empires. In this competition, also by the assimilation process of the imperialist states and also revolution (random changes that suddenly happen in the position of some countries) an increase in the power of colonies will gradually occur and the position of empire and colonies be changed. The process is terminated when only one empire remains and all the weak empires collapse [28].

2.2.3. Artificial neural networks (ANNs)

ANNs, among the most popular AI techniques, have been developed based on the human brain construction [4]. One of the most useful types of these networks is the multi-layer perceptron (MLP) and FFNN network with a back-propagation training algorithm. These networks consist of several mutually processing elements called neurons in three layers including the input layer (number of neurons in this layer is equal to input variables), hidden layer(s) (number of neurons is determined based on the complexity of the problem), and an output layer. According to the previous studies, a network consisting of one or two hidden layer is capable to predict the most complex problems, and also the optimal number of hidden layer neurons is usually determined by trial and error (choosing too many neurons in these layers may result in overfitting, and less neurons will decrease the network performance) [30]. More details on the neural network can be found in the literature [3, 4, 31].

2.2.4. Adaptive neuro-fuzzy inference system (ANFIS)

ANFIS is a multi-layer transmission network that uses the input-output data, learning algorithms of neural networks, and if-then rules of fuzzy in the training process. This algorithm was introduced by Jang in 1993 in which a fuzzy inference system operates within compatible neural networks [22, 30, 32]. In this approach, an empirical knowledge is converted into a mathematical mapping by tye verbal or linguistic rules. However, in the systems where expert knowledge is either not available or not accurately expressed, the neural network method can create the functions that benefit from the membership and system rules [33]. Figure 4 illustrates a schematic view of the ANFIS structure (type 3 ANFIS) with two inputs.

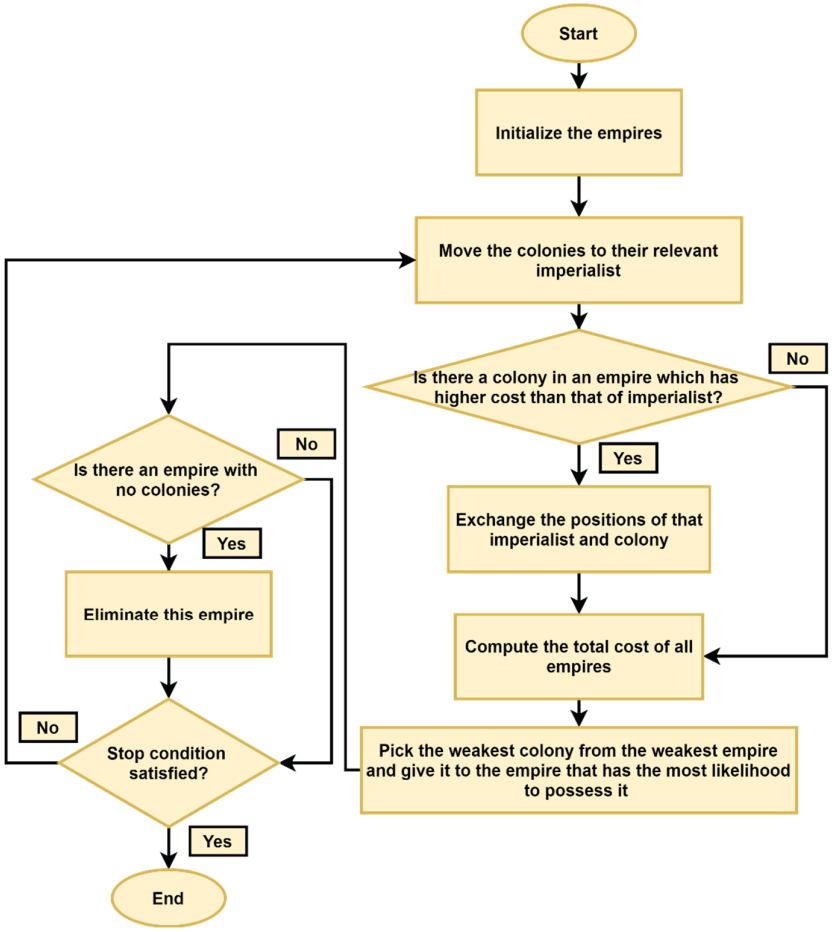

Figure 3. Flowchart of colonial competition algorithm ICA [29].

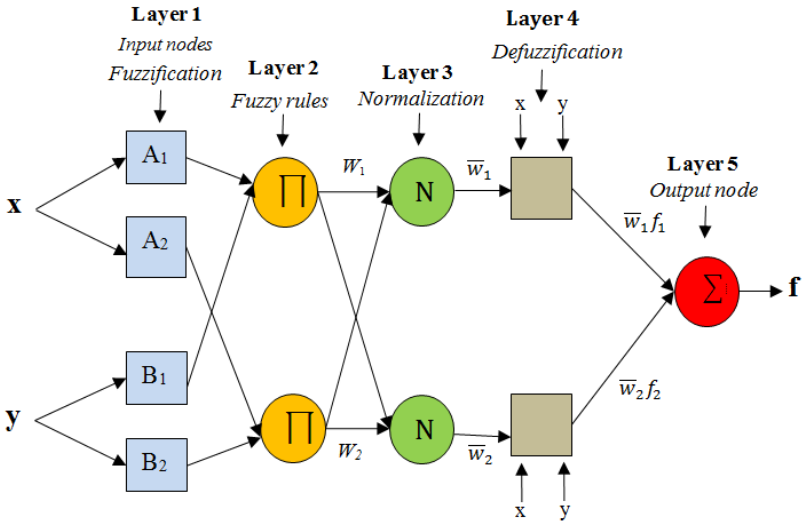

Figure 4. A Schematic view of ANFIS structure including two inputs [32].

According to Figure 4, the structure of the ANFIS model involves five distinct layers. In the first layer, fuzzification occurs by various types of membership functions. In the second layer, the received signals from the first layer are multiplied. In fact, in this layer, the firing strengths for the fuzzy rules are generated. In the third one, the calculated firing strengths are normalized. Defuzzification happens in the fourth layer, and the final outputs of i considered inputs (with attained

weights w_i) are achieved in the fifth layer or output layer by the following equation [19, 34]:

$$Final\ \text{output} = \sum_i \overline{w_i} f_i = \frac{\sum_i w_i f_i}{\sum_i w_i} \quad (6)$$

3. Results and Discussion

3.1. Predicting flyrock by linear multivariate regression model

Table curve software, as a powerful statistical software, was used to extract the best statistical relationship between the considered inputs and the flyrock distance data. These relationships are assessed based on their R-squared coefficients. Thus the linear dependence between the flyrock and the obtained relationships (as the input parameters) was determined by the IBM SPSS software.

The backward statistical analysis was used to determine the multivariate equation. Four statistical parameters including accounted for variance (VAF), mean absolute error (MAE), root-mean-square error (RMSE), and coefficient of determination (R^2) were applied to find the best relationship and prediction in all methods. Finally, Equation 6 with the highest values of 0.9, 90.01, 7.33 m, and 5.15 m for R^2, VAF, RMSE, and MAE, respectively, was extracted for the flyrock prediction using the LMR method.

$$FR = c_1 + \left(\left(c_2 \times B^3\right) + \left(\frac{c_3}{Pf}\right)\right) + \left(\left(c_4 \times B^3\right) + \left(c_5 \times St\right)\right) + \left(\frac{c_6}{D^2}\right) + \left(\left(c_7 \times B \times LN(B)\right) + \left(c_8 \times B^{1.5}\right)\right) \quad (7)$$

where C0 to C8 are the coefficients of Equation 7 listed in Table 3. Hence, the final relationship for predicting the flyrock by considering the inputs is expressed as Equation 8, and comparison of the measured and predicted flyrock values by the LMR relationship is shown in Figure 5.

Table 3. Coefficients of LMR model.

C_1	C_2	C_3	C_4	C_5	C_6	C_7	C_8
307.24	-0.17	-9.45	-0.44	14.22	-366.86	243.57	-195.3

$$FR = 307.24 + \left(\left(-0.17 \times B^3\right) - \left(\frac{9.45}{Pf}\right)\right) + \left(\left(-0.44 \times B^3\right) + \left(14.22 \times St\right)\right) - \left(\frac{366.86}{D^2}\right) + \left(\left(243.57 \times B \times LN(B)\right) + \left(-195.3 \times B^{1.5}\right)\right) \quad (8)$$

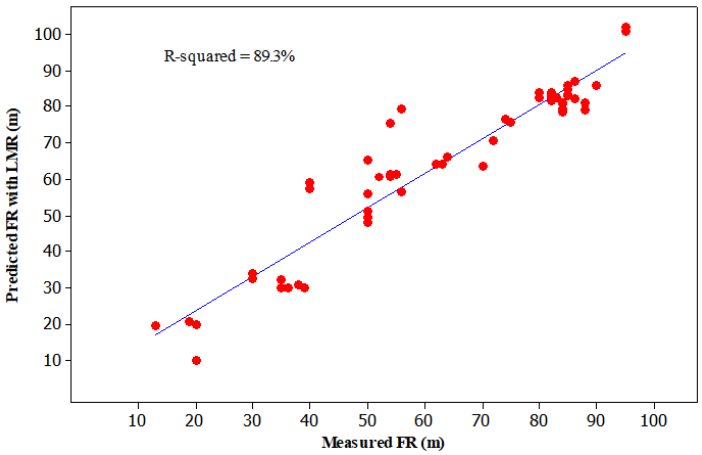

Figure 5. Correlation between measured and predicted flyrock values by LMR.

The relationship between the statistical model validation data and the measured data is shown in Figure 6. This figure shows the error analysis histogram of the proposed model. The error distribution function of the model is normal, suggesting the reliability of the model.

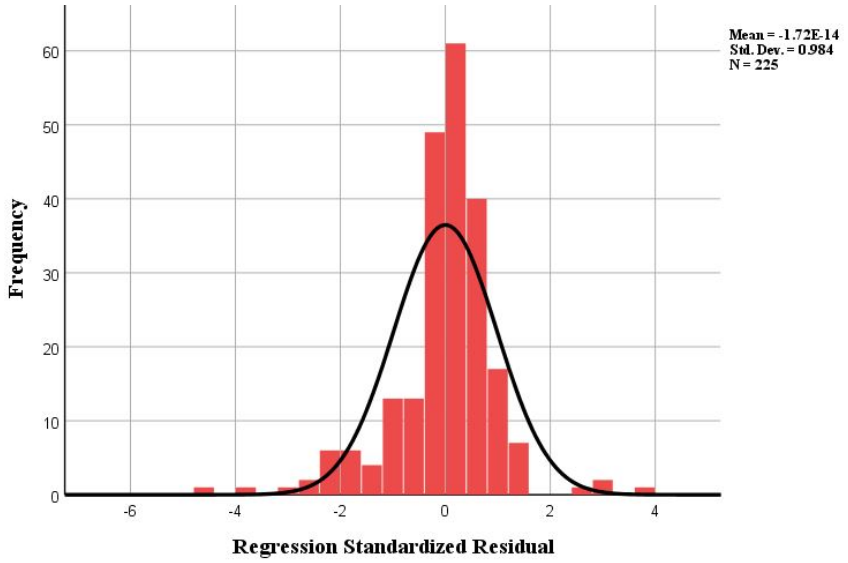

Figure 6. Histogram of presented LMR model error data.

3.2. Optimizing relationship with ICA

In this section, the statistical equation obtained to predict flyrock using the multivariate linear regression method (Equation 8) is optimized by the ICA technique. The optimization process was performed by optimizing the coefficients C0 to C8 in Equation 7. In this algorithm, the functions RMSE and R^2 are considered as the objective functions:

$$\mathrm{RMSE}=\sqrt{\frac{1}{\mathrm{N}}\sum_{\mathrm{i=1}}^{\mathrm{N}}(\mathrm{X_{ipred}}-\mathrm{X_{imeas}})^2} \tag{9}$$

$$\mathrm{R^2}=1-\frac{\sum_{\mathrm{i=1}}^{\mathrm{N}}(\mathrm{X_{imeas}}-\mathrm{X_{ipred}})^2}{\sum_{\mathrm{i=1}}^{\mathrm{N}}(\mathrm{X_{imeas}}-\bar{\mathrm{X}})^2} \tag{10}$$

$$MAE=\frac{1}{n}\sum_{i=1}^{n}\left|x_{imeas}-x_{ipred}\right| \tag{11}$$

where $\mathrm{X_{ipred}}$ is the predicted flyrock, and $\mathrm{X_{imeas}}$ is the measured flyrock distance. Based on the objective functions, the final relation 12, is obtained to predict the blasting-induced flyrock. The optimized coefficients of this relationship are given in Table 4. The values of R^2, RMSE, MAE, and VAF indices for the optimal relationship were 0.91, 7.03 m, 5.19, and 90.63 m, respectively.

Table 4. Optimized coefficients with ICA model.

C_1	C_2	C_3	C_4	C_5	C_6	C_7	C_8
-33.8	20.66	-10.8	-21.64	22.92	-115.846	-99.6	82.98

$$\mathrm{FR}=-33.8+\left(\left(20.66\times\mathrm{B^3}\right)-\left(\frac{10.8}{\mathrm{Pf}}\right)\right)+\left(\left(-21.64\times\mathrm{B^3}\right)+\left(22.92\times\mathrm{St}\right)\right)-\left(\frac{115.85}{\mathrm{D^2}}\right)+\left(\left(-99.6\times\mathrm{B}\times\mathrm{LN(B)}\right)+\left(82.98\times\mathrm{B^{1.5}}\right)\right) \tag{12}$$

For presenting the accuracy and validation of the obtained equations (8 and 12), some of the considered data for testing the models in this work are given in Table 5. The measured relative flyrock distance and the calculated values by these equations are also presented.

Table 5. The measured flyrock and predicted values by LMR and ICA.

D	B	St	Pf	Ch	Flyrock (measured)	Flyrock (LMR)	Flyrock (ICA)
5	4	4.1	0.38	29.5	75	75.672	75.711
5.5	4.5	4.1	0.37	19.2	40	57.209	55.522
5	4.5	4.3	0.36	13.33	56	56.796	58.491
5.5	4.5	4.3	0.44	31.25	62	64.116	64.751
5.5	4.5	3.6	0.36	13.5	50	49.390	43.250
5	4	4.1	0.49	20	84	81.256	82.092
5.5	4	4.1	0.47	20.7	85	82.982	81.958
5.5	5	4	0.29	23.5	19	20.619	20.108
5.5	5	4.5	0.32	16	38	30.783	35.060
4.5	4	4.1	0.36	9.23	72	70.848	73.044
5.5	4.5	4.3	0.44	34.5	63	64.116	64.751
5.5	4.5	4.3	0.38	25	52	60.725	60.874
5.5	4	4.1	0.5	21.37	82	84.188	83.337
5	4	4.1	0.44	52.2	84	79.064	79.587
5.5	4.5	3.6	0.34	13.5	50	47.846	41.485
5.5	5	4.5	0.31	39.6	36	29.830	33.971
5.5	4.4	3.6	0.39	44	50	56.068	49.974
5.5	4	3.2	0.38	15	54	65.423	55.886

In the model produced in MATLAB 2019a, the number of countries, imperialists, and repetitions were 200, 35, and 400, respectively. Figure 7 presents the correlation between the measured and ICA-optimized values of flyrock. Moreover, Figure 8 illustrates the empires created by their colony. Acoording to this figure, the bigger created empires have a greater number of colonies.

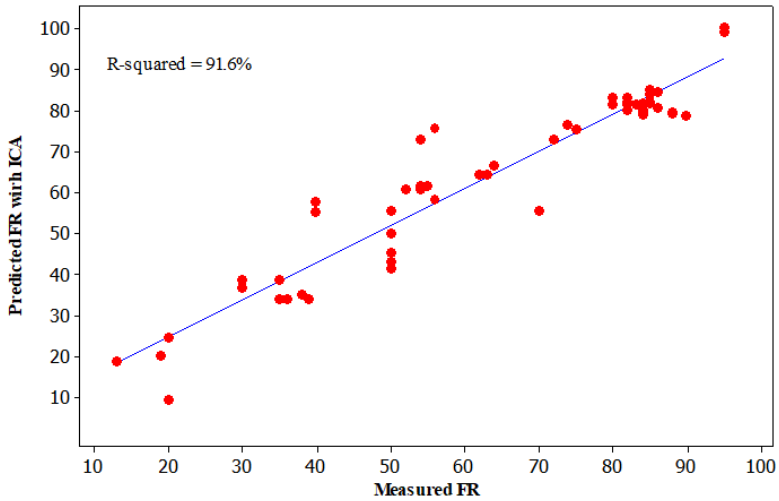

Figure 7. Correlation between measured and ICA-optimized values of flyrock.

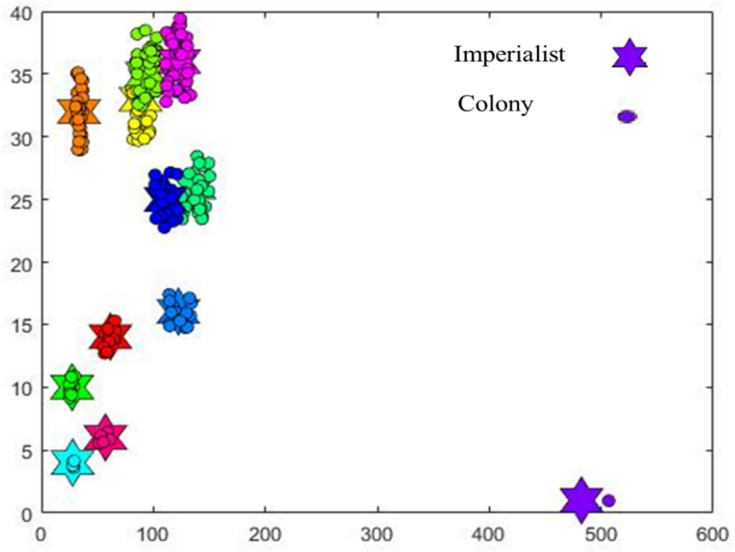

Figure 8. The empires created with their colony in which bigger empires have a greater number of colonies

3.3. Predicting flyrock using ANN

In te present work, ANN was used for flyrock evaluation and prediction. Hence, a feedforward-backpropagation neural network, a type of ANN with high efficiency to predict various problems, was considered. Since the networks with one or two hidden layers can predict more complicated problems, many networks with different structures were applied. Finally, a network with one hidden layer including eight neurons showed the best performance (with the lowest RMSE and highest R^2) in predicting flyrock in this work. To this end, a network with the structure of 5-8-1 (Figure 9), Levenberg-Marquardt as the learning algorithm, and log-sigmoid (logsig) as the transfer function was selected as the optimal network to predict flyrock using the prepared database.

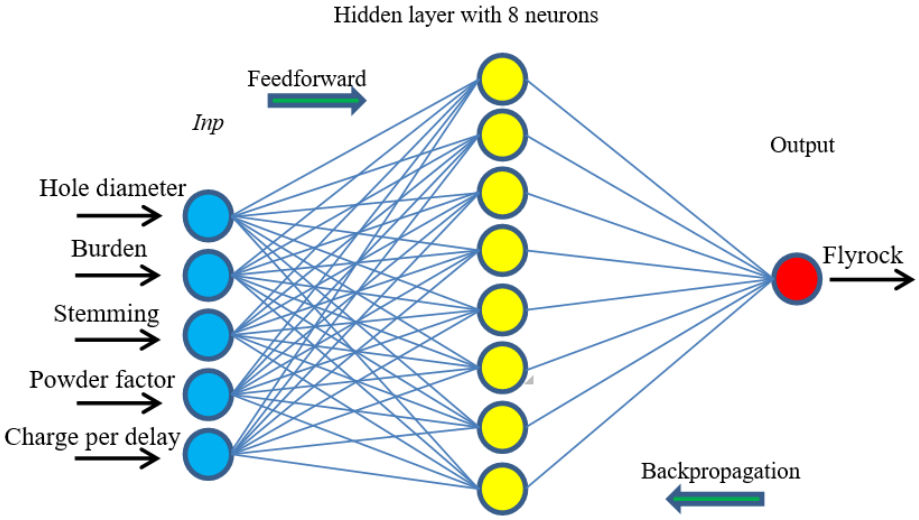

Figure 9. Schematic structure of achieved optimal ANN.

The relationship between the measured flyrock values and the values predicted by ANN for the test data is illustrated in Figure 10. The indicators of RMSE and coefficient of determination (R^2) were considered for assessing the network performance. These values for the selected optimal network were 1.93 m and 99.1% for the train data and 5.04 m and 95.6% for the test data, respectively.

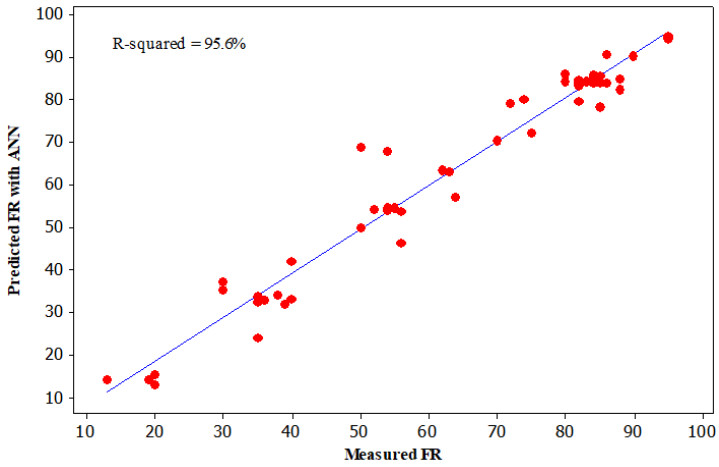

Figure 10. Correlation between measured flyrock and values predicted by ANN.

3.4. Predicting flyrock using ANFIS

The ANFIS method was also used for prediction of the blasting-induced flyrock in present work. Like the ANN method, this method was performed to evaluate and compare the accuracy of the ICA-optimized relationship. The input parameters and data used for the train and test process are considered as the above applied methods. The parameters of the optimum ANFIS for predicting flyrock are listed in Table 6. In addition, Figure 11 shows the correlations of the measured and predicted flyrock values by the ANFIS method.

Table 6. Parameters of optimum ANFIS model.

Parameters	Description/value
Fuzzy structure	Sugeno-type
Membership function for inputs	Gaussian
Membership function for the output	Linear
The influence of cluster centers	0.8
Iteration number	600
Step size for Initializing	0.1
Step size for the decreasing rate	0.7
Step size for the increasing rate	1.3
Fuzzy rules number	5

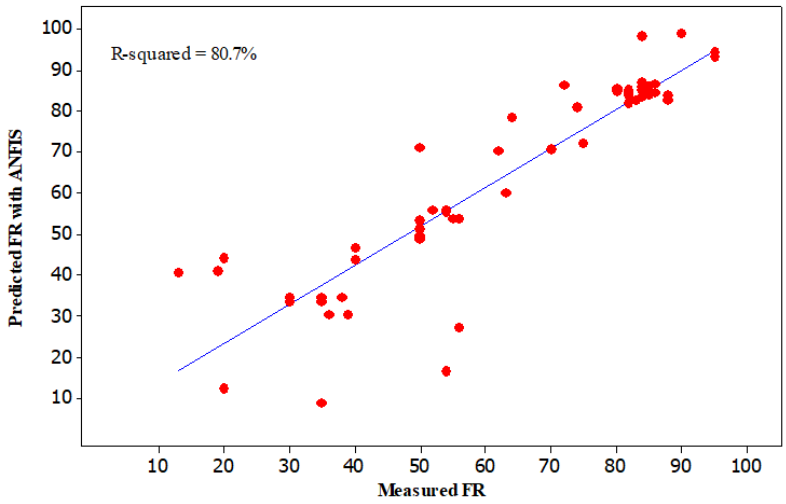

Figure 11. Correlation between measured flyrock and values predicted by ANFIS.

The achieved results of this work presented that the applied methods showed a high ability in prediction of the flyrock (Table 7). Among the considered models, based on the performance indicators for the testing models, the superiority of the ANN model was proved for predicting the flyrock in this work. Evetually, Figure 12 shows a comparison of the values predicted by the intelligent methods and the LMR method used in this work.

Table 7. Results of considered statistical parameters for all optimized models

		Models			
Index		LMR	ICA	ANN	ANFIS
Test	R^2	0.89	0.92	0.96	0.81
	RMSE	7.33	6.85	5.04	10.79
	MAE	5.15	4.92	3.42	5.54
	VAF	0.90	0.91	0.95	0.78

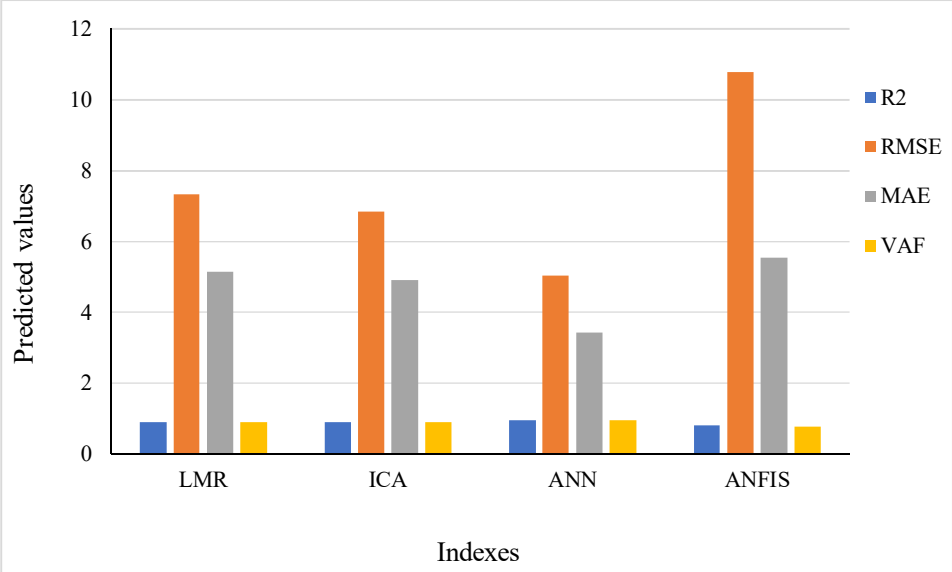

Figure 12. Measured flyrock compared with predicted values by LMR, ICA, ANFIS, and ANN models.

4. Sensitivity Analysis

sensitivity analysis was performed to identify the relative impact of each parameter on the output in the mode using the cosine domain method [35]. All the data pairs were utilized to construct a data array X as follow [35]:

$$X = \{x_1, x_2, x_3, ..., x_i, ..., x_n\} \quad (13)$$

Each one of the elements, xi, in the data array X is a vector of lengths of m, i.e.:

$$X = \{x_1 1, x_2 2, x_3 3, ..., x_{im}\} \quad (14)$$

Equation 15 represents the strength of the relation among the dataset, x_i and x_j:

$$r_{ij} = \frac{\sum_{k=1}^{m} x_{ik} x_{jk}}{\sqrt{\sum_{k=1}^{m} x_{ik}^2 \sum_{k=1}^{m} x_{ik}^2}} \quad (15)$$

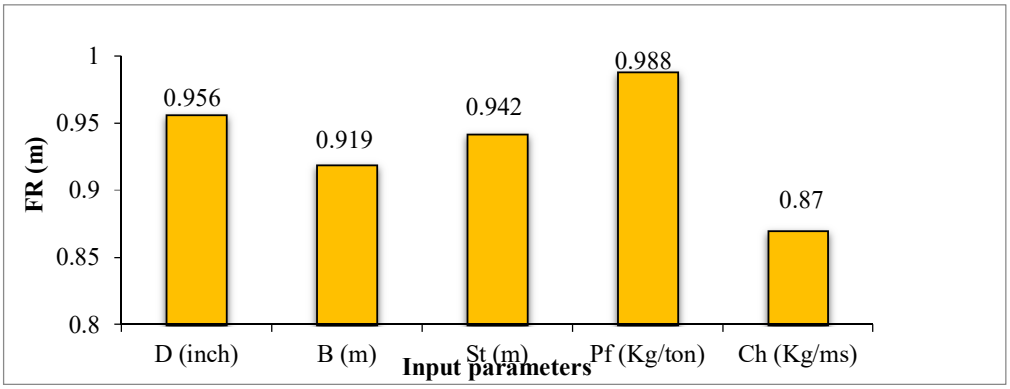

Figure 13. Impact of input parameters on flyrock by sensitivity analysis.

Figure 13 shows the strengths of the relations (r_{ij} values) between the model inputs and outputs. The results obtained showed that the powder factor (Pf), hole diameter (D), stemming (St), burden (B), and charge per delay (Ch) had the most and the least effect on flyrock (FR), respectively.

5. Conclusions

In the present work, different models were applied in order to evaluate and predict the blasting-induced flyrock in the Sungun open-pit copper mine. The parameters of blasthole diameter, burden, stemming, powder factor, and maximum charge per delay were considered as the input parameters of the applied models. The models LMR, ICA, ANFIS, and ANN were applied to predict flyrock in 281 blasting operations in the Sungun copper mine. The performance of these models was compared based on the indicators of R^2, RMSE, MAE, and VAF. According to the achieved results, the values of these parameters for the obtained neural network were 95.6%, 5.04 m, 3.42 m, and 95.27%, respectively. Therefore, the ANN technique was considered as the best model for predicting the flyrock distance. Besides, the results obtained indicated that the ICA technique had a relatively high ability in predicting flyrock, with the LMR and ANFIS being in the following ranks in the order of their appearance. Moreover, the sensitivity analysis showed that powder factor and blasthole diameter had the highest impact on the flyrock phenomenon in the order of their appearance.

References

[1]. Bui, X.N., Nguyen, H., Le, H. A., Bui, H.B. and Do, N.H. (2020). Prediction of blast-induced air over-pressure in open-pit mine: assessment of different artificial intelligence techniques. Natural Resources Research. 29 (2): 571-591.

[2]. Lundborg, N. (1974). The hazards of flyrock in rock blasting. Swedish Detonic Research Foundation Reports, DS 12.

[3]. Monjezi, M., Mehrdanesh, A., Malek, A. and Khandelwal, M. (2013). Evaluation of effect of blast design parameters on flyrock using artificial neural networks. Neural Computing and Applications. 23 (2): 349-356.

[4]. Nguyen, H. and Bui, X.N. (2019). Predicting blast-induced air overpressure: a robust artificial intelligence system based on artificial neural networks and random forest. Natural Resources Research. 28 (3): 893-907.

[5]. Shakeri, J., Shokri, B. J. and Dehghani, H. (2020). Prediction of blast-induced ground vibration using gene expression programming (GEP), artificial neural networks (ANNS), and linear multivariate regression (LMR). Archives of Mining Sciences: 65 (2).

[6]. Nguyen, H., Bui, X.N., Bui, H.B. and Mai, N.L. (2020). A comparative study of artificial neural networks in predicting blast-induced air-blast overpressure at Deo Nai open-pit coal mine, Vietnam. Neural Computing and Applications. 32 (8): 3939-3955.

[7]. Khandelwal, M. and Monjezi, M. (2013). Prediction of backbreak in open-pit blasting operations using the machine learning method. Rock mechanics and rock engineering. 46 (2): 389-396.

[8]. Koopialipoor, M., Fallah, A., Armaghani, D.J., Azizi, A. and Mohamad, E.T. (2019). Three hybrid intelligent models in estimating flyrock distance resulting from blasting. Engineering with Computers. 35 (1): 243-256.

[9]. Ghasemi, E., Sari, M. and Ataei, M. (2014). Development of an empirical model for predicting the effects of controllable blasting parameters on flyrock distance in surface mines. International Journal of Rock Mechanics and Mining Sciences, 52, 163–170.

[10]. Bajpayee, T.S., Rehak, T.R., Mowrey, G.L. and Ingram, D.K. (2004). Blasting injuries in surface mining with emphasis on flyrock and blast area security. Journal of Safety Research. 35 (1): 47-57.

[11]. Lundborg, N., Persson, A., Ladegaard-Pedersen, A. and Holmberg, R. (1975). Keeping the lid on flyrock in open-pit blasting. Engineering and Mining Journal. 176: 95–100.

[12]. Dehghani, H. and Shafaghi, M. (2017). Prediction of blast-induced flyrock using differential evolution algorithm. Engineering with Computers. 33 (1): 149-158.

[13]. Lu, X., Hasanipanah, M., Brindhadevi, K., Amnieh, H. B. and Khalafi, S. (2020). ORELM: A novel machine learning approach for prediction of flyrock in mine blasting. Natural Resources Research. 29 (2): 641-654.

[14]. Rad, H. N., Bakhshayeshi, I., Jusoh, W. A. W., Tahir, M. M. and Foong, L. K. (2020). Prediction of flyrock in mine blasting: a new computational intelligence approach. Natural Resources Research. 29 (2): 609-623.

[15]. Han, H., Armaghani, D.J., Tarinejad, R., Zhou, J. and Tahir, M.M. (2020). Random forest and bayesian network techniques for probabilistic prediction of flyrock induced by blasting in quarry sites. Natural Resources Research, 1-13.

[16]. Nguyen, H., Bui, X.N., Choi, Y., Lee, C.W. and Armaghani, D.J. (2020). A novel combination of whale optimization algorithm and support vector machine with different kernel functions for prediction of blasting-induced fly-rock in quarry mines. Natural Resources Research, 1-17.

[17]. Zhou, J., Aghili, N., Ghaleini, E.N., Bui, D.T., Tahir, M.M. and Koopialipoor, M. (2020). A Monte Carlo simulation approach for effective assessment of flyrock based on intelligent system of neural network. Engineering with Computers. 36 (2): 713-723.

[18]. Monjezi, M., Dehghani, H., Shakeri, J. and Mehrdanesh, A. (2021). Optimization of prediction of flyrock using linear multivariate regression (LMR) and gene expression programming (GEP)Topal Novin mine, Iran. Arabian Journal of Geosciences. 14 (15): 1-12.

[19]. Amini Khoshalan, H., Shakeri, J., Najmoddini, I. and Asadizadeh, M. (2021). Forecasting copper price by application of robust artificial intelligence techniques, Resources Policy, 73, 102239.

[20]. Onyelowe, K. C., Shakeri, J., Amini Khoshalan, H., Usungedo, T.F. and Alimoradi-Jazi, M. (2022). Computational Modeling of Desiccation Properties (CW, LS, and VS) of Waste-Based Activated Ash-Treated Black Cotton Soil for Sustainable Subgrade using Artificial Neural Network, Gray-Wolf, and Moth-Flame Optimization Techniques. Advances in Materials Science and Engineering, 2022.

[21]. Onyelowe, K.C. and Shakeri, J. (2021). Intelligent prediction of coefficients of curvature and uniformity of hybrid cement modified unsaturated soil with NQF inclusion. Cleaner Engineering and Technology, 4, 100152.

[22]. Onyelowe, K.C., Shakeri, J., Amini Khoshalann, H., Salahudeen, A.B., Arinze, E.E. and Ugwu, H.U. (2021). Application of ANFIS hybrids to predict coefficients of curvature and uniformity of treated unsaturated lateritic soil for sustainable earthworks. Cleaner Materials, 1, 100005.

[23]. Atashpaz-Gargari, E. and Lucas, C. (2007). Imperialist competitive algorithm: an algorithm for optimization inspired by imperialistic competition. In 2007 IEEE congress on evolutionary computation (IEEE), 4661-4667).

[24]. Ahmadi, M. A. (2011). Prediction of asphaltene precipitation using artificial neural network optimized by imperialist competitive algorithm. Journal of Petroleum Exploration and Production Technology, 1, 99-106.

[25]. Yazdipour, A. and Ghaderi, M.R. (2014). Optimization of weld bead geometry in GTAW of CP titanium using imperialist competitive algorithm. International Journal of Advanced Manufacturing Technology. 72 (5-8): 619-625.

[26]. Alzoubi, I., Delavar, M., Mirzaei, F. and Arrabi, B.N. (2017). Integrating artificial neural network and imperialist competitive algorithm (ICA), to predict the energy consumption for land leveling. International Journal of Energy Sector Management. 11 (4): 522-540.

[27]. Shokri, B. J., Dehghani, H. and Shamsi, R. (2020). Predicting silver price by applying a coupled multiple linear regression (MLR) and imperialist competitive algorithm (ICA). Metaheuristic Computing and Applications. 1. 1 (1): 101.

[28]. Rajabioun, R., Atashpaz-Gargari, E. and Lucas, C. (2008). Colonial competitive algorithm as a tool for Nash equilibrium point achievement. In International Conference on Computational Science and Its Applications, 680-695. Springer, Berlin, Heidelberg.

[29]. Hasanipanah, M., Amnieh, H.B., Khamesi, H., Armaghani, D.J., Golzar, S.B. and Shahnazar, A. (2018). Prediction of an environmental issue of mine blasting: an imperialistic competitive algorithm-based fuzzy system. International Journal of Environmental Science and Technology. 15 (3): 551-560.

[30]. Shakeri, J., Asadizadeh, M. and Babanouri, N. (2022). The prediction of dynamic energy behavior of a Brazilian disk containing nonpersistent joints subjected to drop hammer test utilizing heuristic approaches. Neural Computing and Applications, 1-16.

[31]. Monjezi, M., Khoshalan, H.A. and Varjani, A.Y. (2012). Prediction of flyrock and backbreak in open pit blasting operation: a neuro-genetic approach. Arabian Journal of Geosciences, 5, 441–448.

[32]. Jang, J.S. (1993). ANFIS: adaptive-network-based fuzzy inference system. IEEE Transaction

on Systems, Man and Cybernetics. 23 (3): 665-685.

[33]. Zounemat-Kermani, M. and Teshnehlab,M. (2008). Using adaptive neuro-fuzzy inference system for hydrological time series prediction, Applied Soft Computing. 8 (2):928-936.

[34]. Akyildiz, O. and Hudaverdi, T. (2020). ANFIS modelling for blast fragmentation and blast-induced vibrations considering stiffness ratio. Arabian Journal of Geosciences 13, 1162.

[35]. Yang, Y. and Zhang, Q. (1997). A hierarchical analysis for rock engineering using artificial neural networks. Rock Mechanics and Rock Engineering. 30 (4): 207-222.

توسعه مدل‌های جدید برای ارزیابی میزان پرتاب سنگ در معادن روباز

جمشید شاکری[1]، حاصل امینی خوشالان[1*]، حسام دهقانی[1,2] مارک باسکومپتا[3] و کندی اونیلو[4]

۱- بخش مهندسی معدن، دانشگاه کردستان، سنندج، ایران
۲- بخش مهندسی معدن، دانشگاه صنعتی همدان، همدان، ایران
۳- بخش مهندسی معدن، دانشگاه پلی‌تکنیک کاتولونیا، بارسلونا، اسپانیا
۴- بخش مهندسی عمران، دانشگاه میشل اوکپارا، نیجریه

ارسال ۲۰۲۲/۰۴/۰۸ پذیرش ۲۰۲۲/۰۴/۲۸

* نویسنده مسئول مکاتبات: h.amini@uok.ac.ir

چکیده

در این تحقیق، مطالعه جامعی به منظور پیش‌بینی پرتاب سنگ به عنوان یک پدیده رایج و نامطلوب ناشی از عملیات آتشباری در معدن‌کاری روباز صورت گرفته است. علی‌رغم در دسترس بودن چندین مدل تجربی برای پیش‌بینی فاصله پرتاب سنگ، پیچیده بودن ارزیابی پرتاب سنگ موجب کاهش کارایی این مدل‌ها شده است. بنابراین، از روش‌های آماری و هوشمند مصنوعی قدرتمند برای پیش‌بینی پرتاب سنگ در معدن مس سونگون در ایران استفاده شده است. برای این منظور، روش رگرسیون چندمتغیره خطی (LMR)، الگوریتم رقابت استعماری (ICA)، سیستم استنتاج عصبی-فازی تطبیقی (ANFIS) و شبکه عصبی مصنوعی برای پیش‌بینی پرتاب سنگ با در نظر گرفتن پارامترهای مؤثر شامل قطرچال، گل‌گذاری، بارسنگ، خرج ویژه و حداکثر خرج در هر تأخیر مورد استفاده قرار گرفته است. با توجه به نتایج به‌دست آمده، شبکه عصبی با ساختار ۵ ورودی، ۸ نرون در لایه پنهان و یک خروجی با الگوریتم یادگیری لونبرگ – مارکوارت (ML) و توابع انتقال لگاریتمی سیگموئید به عنوان بهترین شبکه با مقادیر جذر میانگین مربعات خطا (RMSE) و ضریب همبستگی (R^2) به ترتیب برابر با ۵/۰۴ متر و ۹۵/۶ درصد برای پیش‌بینی پرتاب سنگ انتخاب گردید. همچنین نتایج نشان داد که روش ICA دارای قابلیت نسبتاً بالایی در پیش‌بینی پرتاب سنگ می‌باشد و روش‌های LMR و ANFIS نیز در رده‌های بعدی قرار گرفتند. در نهایت، آنالیز حساسیت نشان داد که پارامترهای خرج ویژه و قطر چال بیشترین تأثیر را بر روی پرتاب سنگ در این تحقیق دارد.

کلمات کلیدی: پرتاب سنگ، رگرسیون چند متغیره خطی، الگوریتم رقابت استعماری، سیستم استنتاج عصبی – فازی تطبیقی، شبکه عصبی مصنوعی.

Corresponding author: h.amini@uok.ac.ir (J. Shakeri).